



Chlorinated holey double-walled carbon nanotubes for relative humidity sensor

Lyubov G. Bulusheva, Vitalii I. Sysoev, Egor V. Lobiak, Yu. V. Fedoseeva, Anna A. Makarova, Marc Dubois, Emmanuel Flahaut, Aleksander V. Okotrub

► To cite this version:

Lyubov G. Bulusheva, Vitalii I. Sysoev, Egor V. Lobiak, Yu. V. Fedoseeva, Anna A. Makarova, et al.. Chlorinated holey double-walled carbon nanotubes for relative humidity sensor. Carbon, 2019, 148, pp.413-420. 10.1016/j.carbon.2019.04.010 . hal-02181559

HAL Id: hal-02181559

<https://hal.science/hal-02181559>

Submitted on 12 Jul 2019

HAL is a multi-disciplinary open access archive for the deposit and dissemination of scientific research documents, whether they are published or not. The documents may come from teaching and research institutions in France or abroad, or from public or private research centers.

L'archive ouverte pluridisciplinaire **HAL**, est destinée au dépôt et à la diffusion de documents scientifiques de niveau recherche, publiés ou non, émanant des établissements d'enseignement et de recherche français ou étrangers, des laboratoires publics ou privés.




Open Archive Toulouse Archive Ouverte (OATAO)

OATAO is an open access repository that collects the work of Toulouse researchers and makes it freely available over the web where possible

This is an author's version published in: <http://oatao.univ-toulouse.fr/23693>

Official URL: <https://doi.org/10.1016/j.carbon.2019.04.010>

To cite this version:

Bulusheva, Lyubov G. and Sysoev, Vitalii I. and Lobiak, Egor V. and Fedoseeva, Yu. V. and Makarova, Anna A. and Dubois, Marc and Flahaut, Emmanuel  and Okotrub, Aleksander V. *Chlorinated holey double-walled carbon nanotubes for relative humidity sensor*. (2019) Carbon, 148. 413-420. ISSN 0008-6223

Any correspondence concerning this service should be sent
to the repository administrator: tech-oatao@listes-diff.inp-toulouse.fr

Chlorinated holey double-walled carbon nanotubes for relative humidity sensor

L.G. Bulusheva^{a, b, *}, V.I. Sysoev^{a, b}, E.V. Lobiak^a, Yu.V. Fedoseeva^{a, b}, A.A. Makarova^c, M. Dubois^d, E. Flahaut^e, A.V. Okotrub^{a, b}

^a Nikolaev Institute of Inorganic Chemistry, SB RAS, 3 Acad. Lavrentiev Ave, 630090 Novosibirsk, Russia

^b Novosibirsk State University, 2 Pirogova Str, 630090 Novosibirsk, Russia

^c Institute of Solid State and Material Physics, Dresden University of Technology, 01062 Dresden, Germany

^d Université Clermont Auvergne, Sigma Clermont, CNRS, ICCF, 24 Blaise Pascal Ave., 63000 Clermont-Ferrand, France

^e CIRIMAT, Université de Toulouse, CNRS, INPT, UPS, UMR CNRS-UPS-INP N° 5085, Université Toulouse 3 Paul Sabatier, Bât. CIRIMAT, 118, route de Narbonne, 31062 Toulouse cedex 9, France

ABSTRACT

A chemical procedure for modification of double walled carbon nanotubes (DWCNTs) to enhance their response to humidity was developed. The DWCNTs walls were etched by hot concentrated sulfuric acid, after what the edge carbon sites were saturated by chlorine via reaction with CCl₄ vapor. This treatment increases the dispersibility of DWCNTs in solvents, removes oxygen groups, and produces chlorine decorated holes in the outer walls. Networks of chlorinated holey DWCNTs showed a high repeatable response to humid environment and a good reversible behavior after the sensor purging by dry air. The density functional theory calculations predict enhanced polarization of the DWCNTs when they contain chlorine decorated holes in the outer walls and physisorption of H₂O molecules near chlorine atoms. These two effects are the cause of an intense low noise signal to gaseous H₂O and easy sensor recovery.

Keywords:

Double-walled carbon nanotubes

Holey nanotubes

Chlorination

Relative humidity sensor

1. Introduction

In the family of carbon nanotubes (CNTs), double walled CNTs (DWCNTs) occupy a place between single walled CNTs (SWCNTs) and multi walled CNTs (MWCNTs) [1]. DWCNTs are composed of two coaxial cylindrical walls, and the inter wall interactions have an impact on their electronic structure and properties, like in MWCNTs [2]. At the same time, the outer walls of DWCNTs have diameters close to SWCNTs and hence possess similar chemical reactivity. During a chemical reaction, the outer walls of DWCNTs protects the inner ones so functionalized DWCNTs maintain most of their electrical conductivity [3,4] and mechanical resistance [5]. This gives advantages for the use of DWCNTs in composites [6,7], electrochemical cells [8,9], biosensors [10] and gas sensors [11].

Humidity sensors are important in industry, medicine, research,

and many everyday life applications. Theoretical calculations predict a weak interaction of water molecules with a perfect CNT surface [12]. The adsorbed H₂O molecule polarizes a SWCNT without any noticeable transfer of electron density between the components [13]. However, changes in the electrical conductivity of CNTs depending on environmental humidity were detected experimentally [14]. The reason for this is mainly the functionalization of the CNTs during purification procedures, and the adsorption of water between junctions in the networks of CNTs. Purification of CNTs using mineral acids produces oxygen containing groups, which interact with water via the hydrogen bonds [15]. This may significantly influence the electrical response of CNTs in case they contain a low amount of defects. Actually, the characterization of a network of purified arc produced SWCNTs revealed a crossover from decreasing to increasing conductance versus H₂O concentration in the surrounding atmosphere [16]. Interestingly, the DWCNTs did not exhibit such a behavior [17]. A large electrical hysteresis measured for a single DWCNT in wet and dry air was assigned to the inter wall interactions. These interactions cause p doping of the outer nanotube, thus increasing its ability to adsorb H₂O molecules.

* Corresponding author. Nikolaev Institute of Inorganic Chemistry, SB RAS, 3 Acad. Lavrentiev Ave, 630090 Novosibirsk, Russia.

E-mail addresses: bul@niic.nsc.ru (L.G. Bulusheva), fedoseeva@niic.nsc.ru (Yu.V. Fedoseeva), marc.dubois@univ-bpclermont.fr (M. Dubois), flahaut@chimie.ups-tlse.fr (E. Flahaut).

Functionalization of the CNTs surface is a way to tailor the sensitivity and selectivity of CNT based sensors to specific analytes [18]. A standard procedure to increase the interaction between a CNT and gaseous H₂O molecules is the grafting of oxygen containing groups to the outer wall. Humidity sensors based on oxygen functionalized CNTs have a fast response followed by a long recovery (usually between 1 and 2 min) [19,20], unfortunately. This can be due in particular to a strong interaction of H₂O with carboxylic groups [15]. Adsorption sites for weaker H₂O bonding are defects in the CNT walls. Theoretical calculations have shown that the Stone Wales defect is attractive for H₂O molecule [21]. Experiments with SWCNTs treated by Ar plasma have evidenced a strong positive effect for sensing of ethanol gas [22], which has a weak electron donation ability similar to water. The plasma treatment produces defects [23] that enhance the sensitivity of the sensor as compared to the non treated sample.

In this paper, we propose a chemical procedure for covalent functionalization of DWCNTs by chlorine and demonstrate the prospect of the material as relative humidity (RH) sensor. Theory predicts a weak interaction of chlorine with large diameter CNTs [24]. Experiments have shown in particular that the treatment of DWCNTs in a Cl₂/O₂ atmosphere at 1000 °C causes no chlorine attachment, but removes metal and disordered carbon contaminations [25]. Covalent C–Cl bonds are formed by using chlorine containing molecules, which can generate chlorine atoms under thermal [26], plasma [27], or ultra violet photolysis [28] activation. The carbon sites reacting with chlorine are defects in CNT walls or CNT edges [27]. Chlorination enhances overlapping of SWCNTs in an entangled network [29] and polarizes the CNT surface [30]. As far as we know, the gas sensing properties of chlorinated CNTs and graphitic materials have not been investigated earlier.

Our strategy consists in the creation of holes in the DWCNTs walls by chemical etching and removal the contaminants from the DWCNTs surface by replacement of oxygen containing groups at the holes boundaries by chlorine atoms using a high temperature treatment by CCl₄ vapor. The first step reduces the contribution of the junction resistance between the DWCNTs in the network. As a result, the sensors response increases, and drift becomes negligible. The second step further contributes to the relative response enhancement and significant decrease in the signal/noise ratio. Calculations performed by density functional theory (DFT) show that the interaction of H₂O molecule with the surface of chlorinated holey SWCNT has a physisorption character. However, the binding energy substantially increases in case of the DWCNTs due to the inter wall interactions.

2. Experimental

2.1. Synthesis

DWCNTs were produced by a catalytic chemical vapor deposition (CCVD) method using a Mg_{1-x}Co_xO solid solution with addition of Mo oxide and a CH₄–H₂ mixture at 1000 °C. The synthesis details are described elsewhere [31]. Accessible catalyst and MgO support were dissolved using a concentrated aqueous HCl solution.

The obtained product is a mixture of disordered carbon (initially deposited on the MgO surface free of the catalyst [32]) and CNTs with a number of walls ranging from one to three and a large predominance of DWCNTs (*ca.* 80%). Disordered carbon was removed using two procedures. The first one was a heating in air at 550 °C for 30 min. In situ Raman spectroscopy study of the oxidation process has evidenced a very low I_D/I_G ratio at this temperature [33]. Following the air oxidation, the sample was cleaned with HCl in order to dissolve Co residues. Hereinafter, the obtained sample is denoted air DWCNTs. The second procedure was etching of the

disordered carbon by concentrated mineral acids. The sample was refluxed at 130 °C in 3 M HNO₃ for 24 h followed by a treatment at 70 °C in 1:3 vol. solution of 15 M HNO₃ and 18 M H₂SO₄ for 5 h. It has been shown that this procedure allows removal of disordered carbon and additionally functionalizes the DWCNTs walls by oxygen containing groups [34].

Holes in the DWCNTs walls were created by boiling the oxidized DWCNTs in concentrated H₂SO₄ for 1 h. When we used this procedure for graphite oxide treatment, the formation of numerous holes with an average size of ~2 nm was observed [35]. At high temperature the acid interacts with oxygen containing groups resulting in the defunctionalization of the basal plane and the development of holes with boundaries saturated by hydrogen and oxygen [36]. The DWCNTs sample after this treatment is denoted h DWCNTs.

Chlorination of air DWCNTs and h DWCNTs was carried out by CCl₄ vapor at 650 °C for 15 min. The details of the synthesis are presented elsewhere [37]. The obtained samples are denoted Cl air DWCNTs and Cl h DWCNTs.

2.2. Characterization methods

Transmission electron microscopy (TEM) characterization of the samples was performed on a JEOL JEM ARM200F microscope equipped with a Cs aberration corrector. An acceleration voltage of 200 kV was used for recording TEM and high angle annular dark field (HAADF) scanning TEM (STEM) images.

X ray photoelectron spectra (XPS) were recorded using monochromatic radiation of 830 eV at the Russian German beamline of the Berliner Elektronenspeicherring für Synchrotronstrahlung (BESSY II), Helmholtz Zentrum Berlin. The content of elements was evaluated from the ratio of the area under the corresponding core level peaks taking into consideration the photoionization cross sections at the given photon energy and transmission function of the analyzer. The energy scale was calibrated to the Au 4f_{7/2} peak at 84 eV. The background signal was subtracted by Shirley's method.

Electron paramagnetic resonance (EPR) spectra were recorded using a X Band Bruker EMX spectrometer equipped with a standard variable temperature accessory and operating at 9.653 GHz. Diphenylpicrylhydrazyl (DPPH) (*g* = 2.0036 ± 0.0002) was used to calibrate the resonance frequency. In order to avoid distortion of the spectrum, the modulation amplitude of the static field was maintained at less than or equal to one third of the smallest peak to peak linewidth (ΔH_{pp}) each time. Non saturated microwave power levels were used when determining the *g* values and ΔH_{pp}. Data processing was performed using Bruker WIN EPR and Sim Fonia software, respectively.

2.3. Sensor preparation and testing

Pulsed ultrasound with a power of 100 W was used to disperse DWCNTs in an aqueous solution of sodium dodecyl sulphate (SDS, 1 wt %). A tip with a diameter of 5 mm has operated with amplitude 30% for 30 min in order to achieve splitting of bundles and to prevent further functionalization of the DWCNTs. The concentration of DWCNTs powder in the solvent was 0.02 mg mL⁻¹. The suspensions were vacuum filtered through cellulose nitrate (CN) membranes with a pore size of 0.45 μm. A rectangular piece of the CN membrane was then placed on a glass substrate (sample in contact with the glass) and pressed at 90 °C for 30 min. This ensures good adhesion of the DWCNT film to the substrate. The CN membrane was dissolved using acetone, then the supported DWCNT film was washed with acetone and dried under ambient conditions. Finally, the samples were cut into 3 × 5 mm sized pieces and glued with 1 mm thick contact pads using RS (UK) silver

conducting paste.

The sensors tests were performed at room temperature using a flow chamber described in detail elsewhere [38]. Dry argon or dry air ($C_{H_2O} < 300$ ppm) passed through a flask with deionized water to produce a wet gas flow. Dry gas and wet gas were mixed at different ratios using mass flow controllers. The total gas flow rate in all experiments was 150 mL min^{-1} . The sensor's resistance was determined by means of a Keithley 6750 picoammeter at a constant voltage of 25 mV. A conventional test consisted of exposure to a dry gas flow in order to determine a baseline resistance, exposure to a wet flow (up to RH 100%), and finally regeneration of the sensor using a dry gas flow. The sensor's response was defined as:

$$\text{Response} = \frac{R_g - R_0}{R_0} \quad (1)$$

where R_0 is the starting resistance, R_g is the resistance measured under gas/humidity atmosphere.

2.4. DFT calculations

The calculations were made using the gradient corrected functional of Perdew–Burke–Ernzerhof (PBE) with local and nonlocal exchange and correlation [39] as implemented in the program package Jaguar (Jaguar, version 7.9, Schrodinger, LLC, New York, NY, 2012). Atomic orbitals were presented by the 6-31G basis set.

We took a fragment of armchair (9,9) CNT to model an outer wall of a DWCNT. This nanotube has a diameter of $\text{ca. } 12.3 \text{ \AA}$, which is the minimum value established from the TEM study of the DWCNTs [31]. The (9,9) nanotube is able to nest the (4,4) carbon nanotube [40]. The CNT models had a length of $\text{ca. } 22.2 \text{ \AA}$ and hydrogen atoms saturated the dangling carbon bonds at the edges. Geometry optimizations were performed with default convergence criteria. The absence of imaginary frequencies indicated that the obtained structures correspond to the local minima on potential energy surfaces. At first, we have fully optimized the (4,4) nanotube fragment. Then, the obtained nanotube has been placed into the center of the (9,9) nanotube fragment and the latter nanotube was optimized at frozen inner nanotube. The relaxed structure was used to create holey CNT models. For these models (without and with adsorbed H_2O), positions of the atoms located at a distance of more than 6 \AA from the hole boundary were not optimized. The models based on (4,4)@(9,9) DWCNT were constructed by combining the optimized components.

The adsorption energy of a H_2O molecule on ideal or holey CNT fragments was calculated as $E_{\text{ad}} = E_{\text{tot}}(\text{CNT}) + E_{\text{tot}}(H_2O) - E_{\text{tot}}(\text{model})$, where $E_{\text{tot}}(\text{CNT})$, $E_{\text{tot}}(H_2O)$ and $E_{\text{tot}}(\text{model})$ are the total energy of the isolated CNT fragment, the isolated H_2O molecule, and the model with adsorbed H_2O , respectively. Atomic charges were calculated by the Natural Bond Orbital (NBO) analysis.

3. Results and discussion

3.1. Materials structure and composition

We have compared three materials: (1) air DWCNTs, obtained by the heat treatment of raw, as synthesized sample in air, (2) h DWCNTs with oxygen decorated holes in the walls, and (3) Cl h DWCNTs produced by the high temperature CCl_4 treatment of h DWCNTs.

XPS analysis showed that the conventional purification procedure of a DWCNT sample by heating in air results in attachment of $\text{ca. } 5 \text{ at. \%}$ of oxygen (Fig. S1 in Supporting Information). Analysis of the C 1s and O 1s spectra (Fig. 1) shows that most of the oxygen is in the form of carboxyl groups [41]. The component in the C 1s

spectrum located around 285.3 eV corresponds to defects and C–H bonds [42]. The content of oxygen increases to $\text{ca. } 12 \text{ at. \%}$ in the h DWCNTs (Fig. S1) and this oxygen forms different functional groups (Fig. 1), particularly, hydroxyls and carboxyls [43]. The C 1s spectrum of this sample has an enhanced intensity of the component at $\sim 285.3 \text{ eV}$, which could confirm the creation of defects (holes) in the DWCNTs walls as result of the boiling in concentrated H_2SO_4 .

The treatment of the h DWCNTs by CCl_4 vapor removed almost all the oxygen and attached $\text{ca. } 4 \text{ at. \%}$ of chlorine (Fig. S1). Moreover, EPR data showed a significant decrease in the content of residual metal after such treatment (Fig. S2). Because of a linewidth of about 1100 G and a g factor of 2.1 , the EPR signal is assigned to residual metallic catalysts (Co) rather than carbon dangling bonds or conduction electrons. For those latter cases, narrow line, i.e. several Gauss, with g of 2.003 is expected. EPR has been often used to highlight the efficiency of catalyst removal [44,45]. Spectra recorded in air and under vacuum being similar, no interaction with paramagnetic O_2 occurs that must result in changes on linewidth and intensity.

The component related to defects in the C 1s spectrum of the Cl h DWCNTs has a very similar intensity compared to the starting h DWCNT sample (Fig. 1). Occurrence of the holes in the DWCNT walls can explain the large amount of chlorine in this sample. XPS Cl 2p spectrum consists of a single doublet, where the position of $2p_{3/2}$ spin orbit component at 200.6 eV (Fig. 2(a)) corresponds to the bonding of chlorine with edge carbon atoms at a graphene fragment [46,47]. The holes can serve as channels for the penetration of chlorine inside the DWCNT. Actually, the HAADF/STEM image of a Cl h DWCNT exhibits bright spots inside the nanotube (Fig. 2(b)), which are likely to be encapsulated chlorine species.

A control experiment with CCl_4 treatment of air DWCNTs resulted in the attachment of $\text{ca. } 1 \text{ at. \%}$ of chlorine only (Fig. S1) and the Cl 2p spectrum found that only 60% of this chlorine was involved in covalent C–Cl bonds (Fig. 2(a)). These bonds can develop at the ends of DWCNTs, which have been open during the heating in air. The importance of edged carbon atoms for chlorination of DWCNT sample is demonstrated by the data showing no chlorine in the as produced DWCNT based sample treated by Cl_2 flow at temperatures of $900\text{--}1110^\circ\text{C}$ [25].

TEM images of the investigated samples show a splitting of the DWCNTs bundles resulting from the acidic treatment (Fig. 3). The size of the bundles decreases from 10 to 20 nm in air DWCNTs (Fig. 3(a)) to $3\text{--}10 \text{ nm}$ in Cl h DWCNTs (Fig. 3(b)). This is important for the nanotube network resistance, as we will discuss later.

3.2. Sensors study

Before the sensor's tests, we have measured the resistance of the DWCNT based networks. To remove the residual solvent, each sample was dried at 100°C for 30 min and then flushed with dry argon for an hour. The obtained resistance value was $\sim 1 \text{ k}\Omega$ for air DWCNTs, $\sim 0.06 \text{ k}\Omega$ for h DWCNTs, and $\sim 0.4 \text{ k}\Omega$ for Cl h DWCNTs. Conducting channels in the networks are formed via connections of neighboring nanotubes [48]. The resistance of an entangled CNT network is determined by the electronic properties of individual CNTs and the resistance at CNT junctions. The latter contribution prevails when the CNTs have a low defect density, such as our air purified DWCNTs. The treatment by acids used in the preparation of h DWCNTs and Cl h DWCNTs creates defects in the walls of the DWCNTs. Since the Raman spectra reveals a similar density of defects in h DWCNTs and Cl h DWCNTs (Fig. S3), the higher resistance of the latter network is attributed to better splitting of bundles as observed from TEM images (Fig. 3). In fact, previous experiments have shown that CNT network conductivity decreases with the mean bundle diameter [49].

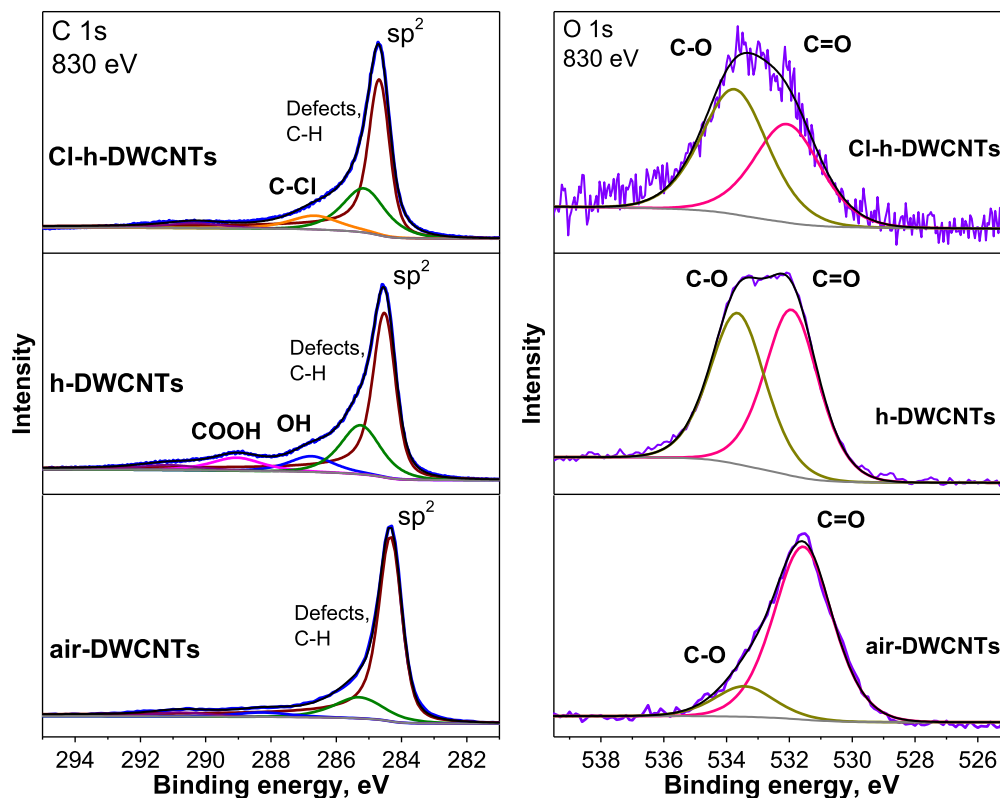


Fig. 1. XPS C 1s and O 1s spectra of air-purified DWCNTs (air-DWCNTs), holey DWCNTs (h-DWCNTs), and chlorinated holey DWCNTs (Cl-h-DWCNTs). (A colour version of this figure can be viewed online.)

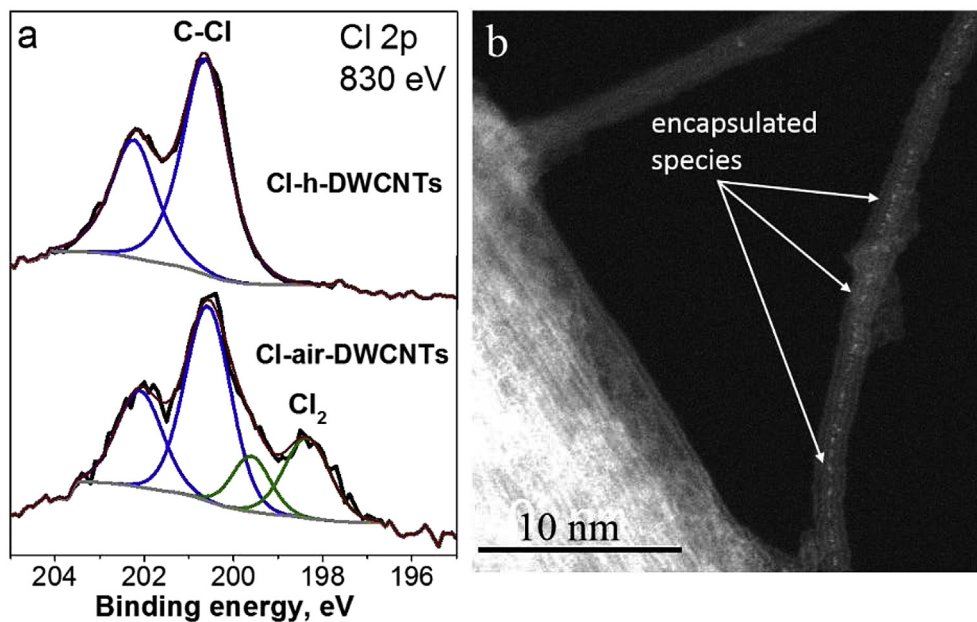


Fig. 2. a) Comparison of XPS Cl 2p spectra of chlorinated air-purified DWCNTs and holey DWCNTs. b) HAADF/STEM image of chlorinated holey DWCNTs (Cl-h-DWCNTs). (A colour version of this figure can be viewed online.)

We first tested the sensors in wet argon in order to study the H_2O sensing mechanism of DWCNT based networks in the absence of other active air molecules. The dynamic tests at a constant RH (100%) followed by exposure to Ar flow is presented in Fig. 4. All sensors have a good stability starting from the third cycle. The air DWCNTs showed the smallest relative response of about 4%,

characteristic of the oxidized CNTs [15]. The response substantially increased for the h DWCNTs. This is because the resistance of this network is determined by the changes in the resistance of the defective nanotubes, while the contribution from the inter tube junctions is small [50]. However, the signal was very noisy. The reason could be a poor contact between surfaces of highly oxidized

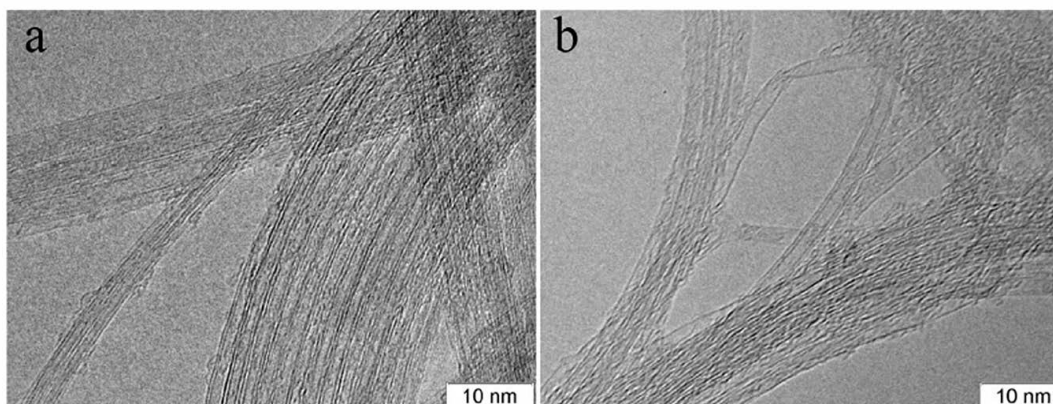


Fig. 3. a) TEM images of air-purified DWCNTs and b) chlorinated holey DWCNTs.

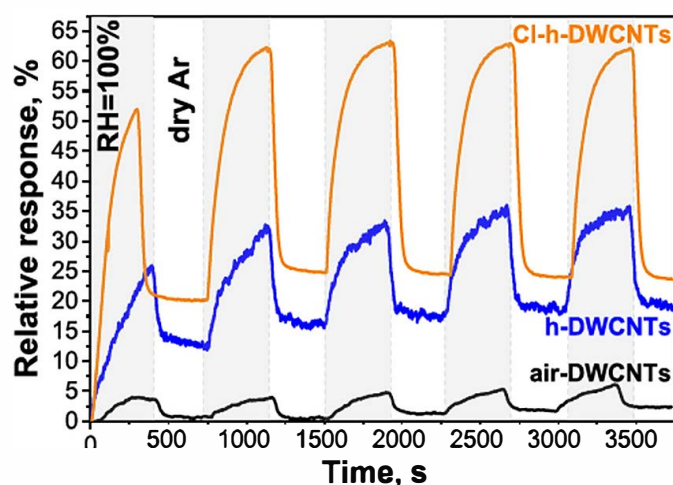


Fig. 4. Dynamic adsorption/desorption response of air purified DWCNTs (air-DWCNTs), holey DWCNTs (h-DWCNTs), and chlorinated holey DWCNTs (Cl-h-DWCNTs) in argon saturated with water vapors. (A colour version of this figure can be viewed online.)

nanotubes. The air DWCNT and h DWCNT sensors exhibited a small drift due to trapping of H₂O molecules between the nanotubes [51]. A step like shape of the signals recorded for these sensors could reveal the existence of two kinds of adsorption sites, namely, the surface oxygen groups and the inter tube junctions. The latter kind of adsorption sites gives a significantly smaller contribution to the performance of the Cl h DWCNT sensor as follows from the rapid saturation of the signal and the absence of the drift starting from the second target exposure. The high temperature treatment used for the preparation of Cl h DWCNTs removes almost all oxygen from the nanotube surface and the cleaned defective nanotubes contact strongly, that hinders penetration of H₂O molecules between them.

The characteristics of the sensors averaged over four cycles following the first adsorption/desorption are collected in Table 1. All sensors were characterized by the same recovery time, which is

close to those observed for oxidized MWCNTs [52] and graphene materials [53]. Among the studied samples, the Cl h DWCNTs have the highest relative response and the lowest response time toward H₂O vapor. Moreover, this sensor showed a repeatable stable response in air saturated with water vapor (Fig. S4). The sensor responds much faster to humid air than to wet argon, while the sensor's recovery time is almost independent of the environment (Table 1). This result indicates that Cl h DWCNTs have a prospect for monitoring of relative humidity.

Operation capabilities of the Cl h DWCNT sensor in practical conditions were further identified from measurements at various RH levels. The conductivity of the sensor drops gradually with an increase in the air humidity (Fig. 5(a)). Since the initial Cl h DWCNTs are p doped, such a behavior indicates that the H₂O molecules act as an electron donor for the Cl h DWCNTs. The subsequent decrease in humidity does not lead to the restoration of the initial state of the sensor. Such a behavior corresponds to the joint presence of low energy or reversible and high energy or irreversible sites for H₂O adsorption. The high energy sites are likely pores always present in a CNT network. To extract H₂O molecules from them, the sensor should be heated in dry argon flow at a temperature of $\approx 115^\circ\text{C}$ (Fig. S5). Note, that this temperature is much lower than the value of 165°C for MWCNT based sensor [54] and 220°C for SWCNTs [16]. It has been shown, that chlorinated SWCNTs are stable under oxidative atmosphere up to 1000°C due to a protective effect from chlorine [55]. Therefore, a heating in dry air can be used to restore the Cl h DWCNT sensor. Alternatively, the practical application of the sensor can start after the filling of high energy sites by air molecules. We believe that tightly bound molecules should not interfere with further work of the sensor. Actually, the hysteresis decreases at the second exposure of the sensor to humid air (Fig. 5(a)).

A dependence of the sensor response versus RH was determined from the measurements carried out at the same time (120 s) of exposure to air (Fig. 5(b)). The dependence has a monotonic character and is perfectly fitted by a straight line in log log scale (insert in Fig. 5(b)). Observations of a non linear increase in resistance of MWCNT based sensors with humidity were attributed to difficulty

Table 1
Sensor characteristics of air purified DWCNTs, holey DWCNTs, and chlorinated holey DWCNTs determined at 100% environment humidity.

Material (environment)	Response time, s	Recovery time, s	Relative response, %
air-DWCNTs (Ar)	204	32	4
h-DWCNTs (Ar)	192	31	15
Cl-h-DWCNTs (Ar)	161	31	30
Cl-h-DWCNTs (air)	100	28	29

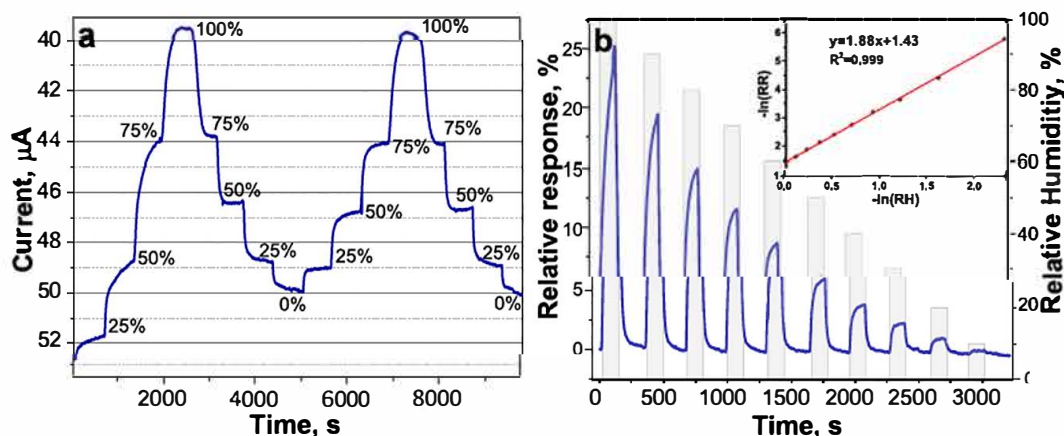


Fig. 5. Tests of the Cl-h-DWCNT sensor in air: (a) variation in electrical current at different relative humidity levels and (b) relative response to target exposure (120 s). The inset shows dependence of sensor relative response on the relative humidity in logarithmic scale. (A colour version of this figure can be viewed online.)

of charge transfer at high humidity levels [56,57]. Zhang and co authors have explained this difficulty by an increased separation of crosslinking CNTs [51], suppressing the mobility of the carriers via the networks [58].

3.3. H_2O adsorption on holey CNTs

To reveal the effect of the holes in the CNT walls on the adsorption of a H_2O molecule, we have invoked the DFT calculations of different models. First, we checked the validity of the PBE/6-31G approach on an example of the non-modified (9,9) CNT fragment. The molecule is oriented by hydrogen atom to the nanotube surface (Fig. S6), giving an adsorption energy of 0.087 eV. This energy perfectly matches with the values of 0.080 ± 0.019 eV for a zigzag (10,0) carbon tube and of 0.070 ± 0.010 eV for graphene, which have been obtained using diffusion Monte Carlo method [12]. This method is able to capture weak interactions due to inclusion of electron correlation and exact exchange. The use of dispersion corrections and Van der Waals inclusive functionals overestimates the adsorption energy for H_2O by about 30–40% [12]. The NBO analysis gives the charge of $-0.0014e$ on the adsorbed H_2O , which agrees well with other calculations, predicting a very weak interaction between a CNT and water [13,59].

A hole in the (9,9) CNT wall was obtained by removal of a central hexagon. When a H_2O molecule approaches close to the hole (Fig. S7(a)), it spontaneously dissociates with the formation of C–O and C–H bonds (Fig. S7(b)). This process continues until all dangling bonds at the hole's boundary become saturated (Fig. S7(c,d)). Thus, an exposure of holey CNTs to water vapor should result in the decoration of the holes by hydrogen and oxygen containing functional groups. This is supported by EPR, which has observed no dangling carbon bonds in the studied materials.

In the next step, we have investigated an interaction of a H_2O molecule with hydrogenated, oxygenated, and chlorinated holes. The resulting configurations, obtained after the optimization of the geometry of the models, are shown in Fig. 6. The H_2O molecule is oriented in such a way as to form the largest number of contacts with hydrogen and oxygen containing functionalities. Thus, it stabilizes in the center of the fully hydrogenated hole (Fig. 6(a)) at a distance of 2.43–2.63 Å from the hydrogen atoms. The molecule forms two hydrogen bonds with the ketone groups (Fig. 6(b)), with the contacts $HOH \cdots O=C$ of 1.95 Å, and with the hydroxyl groups (Fig. 6(c)) via a hydrogen atom ($HOH \cdots O-H$, 1.89 Å) and oxygen ($H_2O \cdots H-O$, 1.60 Å). For the model with a carboxylic group, only

one contact close to the hydrogen bond is found. It is formed by interaction via O–C(OH) species with a hydrogen atom of H_2O . The stronger interaction between the H_2O molecule and the hole is found in the case when hydroxyl and carboxyl groups are simultaneously present at the hole's boundary (Fig. 6(c)). This is due to the realization of very short contacts $H_2O \cdots H-O$, 1.46 Å and $HOH \cdots O=C(OH)$, 1.64 Å. The adsorption energy of H_2O at the chlorinated hole is substantially lower (Fig. 6(f)) than the values characteristics of the hydrogen bonds. The NBO analysis detects a small negative charge q ($-0.008e$) on the chlorine atoms, which causes the orientation of the adsorbed molecule by a hydrogen atom to a chlorine one. The distance between the atoms is ca. 2.74 Å.

Our calculations predict that the H_2O molecule, when adsorbed on a holey CNT, should have a positive charge. Therefore, it donates an electron density to the nanotube. The determined NBO charge, however, is small and varies from $+0.008e$ to $+0.067e$, depending on the functionalities at the hole boundaries (Fig. 6). For the chlorinated holey CNT, the transferred charge of $0.015e$ is a reasonably large considering the small adsorption energy of the H_2O molecule.

The inner nanotubes may influence the interaction of H_2O molecules with the DWCNTs. The walls of a DWCNT are polarized due to redistribution of charge density [60]. Depending on the chirality of the constituting nanotubes, the charge transfer from the outer wall to the inner one ranges from 0.005 to $0.035 e \text{ Å}^{-1}$ [40].

To evaluate the effect of the holes in the outer walls on the reactivity of DWCNTs, we calculated the energies of H_2O adsorption on the fragments of ideal (4,4)@(9,9) nanotube and that containing a functionalized hole. The inner (4,4) nanotube slightly affects the adsorption energy for the ideal DWCNT and the DWCNTs where the hole boundary is decorated by hydrogen and chlorine atoms (Table S1). However, for the oxygen containing DWCNTs the adsorption energy grows by 15–30% as compared to the SWCNT analogs. This can explain the observation of a higher sensitivity of the DWCNTs to H_2O molecules as compared to SWCNTs [17]. Preparations of sensor elements usually include the steps of CNT purification and dispersion, which may introduce in the nanotube walls defects and oxygen groups active to H_2O molecules.

Our calculations confirm negative charging of the inner nanotube in the (4,4)@(9,9) DWCNT (Table S1). The value of the charge transfer of $0.014 e \text{ Å}^{-1}$ well agrees with the literature data [40]. Creation of a hole in the outer nanotube decreases polarization of the DWCNTs, especially for the oxygenated holes. The decoration of the hole's boundary with chlorine atoms has a little effect on the interaction of outer and inner nanotubes. The charge transfer in this

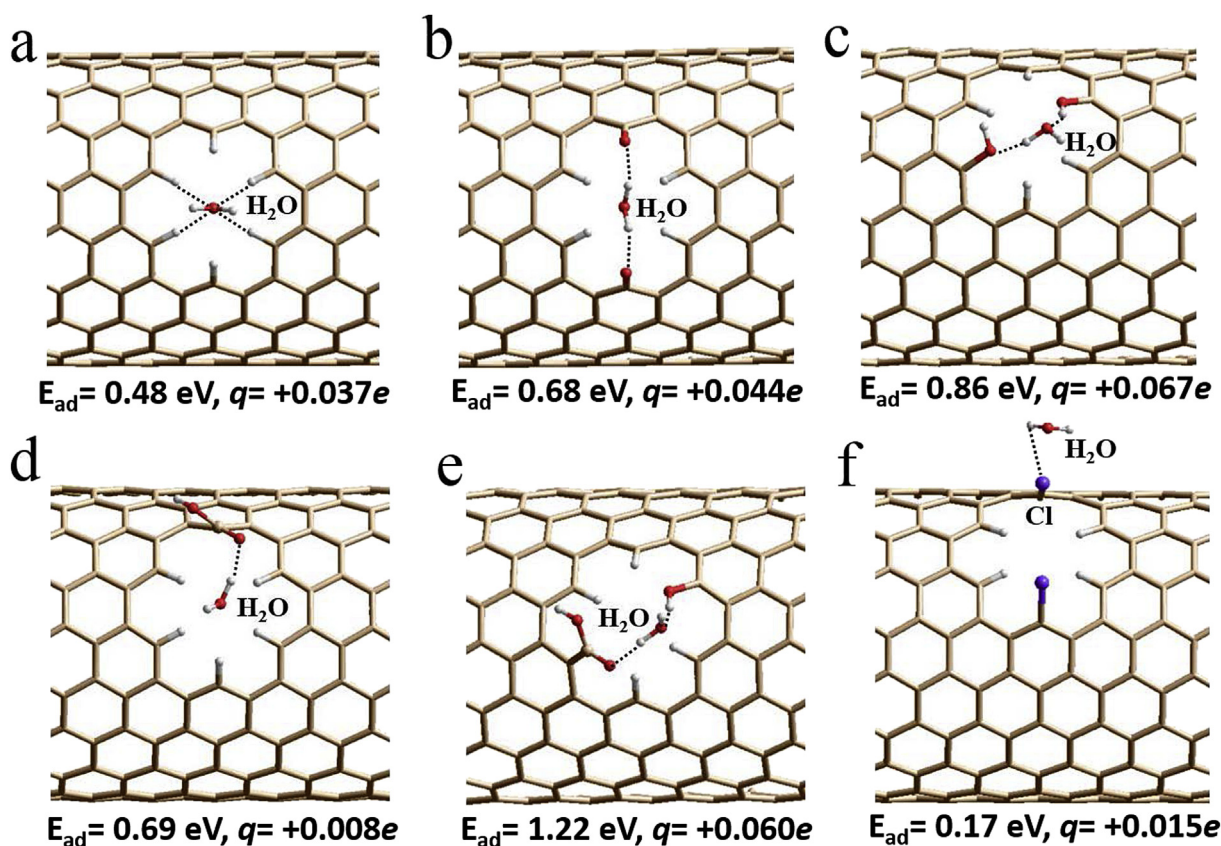


Fig. 6. Optimized position of H_2O molecule at the hole in the (9,9) CNT, decorated by a) hydrogen (white balls) and b) two ketone groups, c) two hydroxyl groups, d) carboxyl group, e) hydroxyl and carboxyl groups, and f) two chlorine atoms (violet balls). The calculated values of the adsorption energy of H_2O and the NBO charge of H_2O . The dot lines show the shortest distances between H_2O and functional groups. (A colour version of this figure can be viewed online.)

DWCNT is $0.012 e \text{ \AA}^{-1}$. Based on the calculation results, we speculate that the Cl h DWCNTs have the conductivity close to that for perfect DWCNTs, but unlike these nanotubes possess a higher reactivity to H_2O molecules. This is the cause of an intense low noise signal to gaseous H_2O . The oxygenation of the holes in the h DWCNTs reduces the nanotubes polarization, which likely leads to a small change in sensor conductivity upon the H_2O adsorption/desorption.

4. Conclusions

We have developed an effective humidity sensor using chemically treated DWCNTs. An oxidation of the DWCNTs by mineral acids splits the bundles that allows forming networks with many more contacts between the nanotubes. Thin films consisting of uniformly distributed DWCNTs possess a low electrical resistance. Boiling the oxidized DWCNTs in concentrated sulfuric acid creates holes in the walls, which serve as adsorption sites for H_2O molecules. Moreover, the contribution of the junctions between adjacent defective nanotubes has a little effect on the total resistance of the network. This considerably increases the response of the DWCNTs sensor. However, the nanotubes functionalized with oxygen containing groups should strongly interact with H_2O molecules, as predicted by DFT calculations. Trapping of the molecules in the oxidized holey DWCNT network results in the drift and the noise of the sensor's signal. The high temperature treatment of these nanotubes by CCl_4 removes oxygen and decorates the holes' boundaries by chlorine. This last treatment significantly improves the relative response of the DWCNTs to H_2O molecules and makes the sensor signal stable and reproducible after the heating at a

relatively low temperature. Based on the calculations, we relate such behavior with a low adsorption energy of H_2O at the chlorinated holes, which, however, is accompanied by a charging of the DWCNTs.

Acknowledgments

The work has been financially supported by the Russian Foundation for Basic Research (Grant № 16 53 150003) and PRC CNRS/RFBFR (Grant No 1023). This research project has been supported by the Russian German Laboratory of BESSY II.

Appendix A. Supplementary data

Supplementary data to this article can be found online at <https://doi.org/10.1016/j.carbon.2019.04.010>.

References

- [1] Y.A. Kim, K.-S. Yang, H. Muramatsu, T. Hayashi, M. Endo, M. Terrones, M.S. Dresselhaus, Double-walled carbon nanotubes: synthesis, structural characterization, and application, *Carbon Letters* 15 (2014) 77–88.
- [2] K.E. Moore, D.D. Tune, B.S. Flavel, Double-walled carbon nanotube processing, *Adv. Mater.* 27 (2015) 3105–3137.
- [3] Y. Piao, C.-F. Chen, A.A. Green, H. Kwon, M.C. Hersam, C.S. Lee, G.C. Schatz, Y. Wang, Optical and electrical properties of inner tubes in outer wall-selectivity functionalized double-wall carbon nanotubes, *J. Phys. Chem. Lett.* 2 (2011) 1577–1582.
- [4] A.H. Brozena, J. Moskowitz, B. Shao, S. Deng, H. Liao, K.J. Gaskell, Y. Wang, Outer wall selectively oxidized, water-soluble double-walled carbon nanotubes, *J. Am. Chem. Soc.* 132 (2010) 3932–3938.
- [5] S. Kawasaki, Y. Kanamori, Y. Iwai, F. Okino, H. Touhara, H. Muramatsu, T. Hayashi, Y.A. Kim, M. Endo, Structural properties of pristine and fluorinated

- double-walled carbon nanotubes under high pressure, *J. Phys. Chem. Solids* 69 (2008) 1203–1205.
- [6] Y.C. Jung, D. Shimamoto, H. Muramatsu, Y.A. Kim, T. Hayashi, M. Terrones, M. Endo, Robust, conducting and transparent polymer composites using surface-modified and individualized double-walled carbon nanotube, *Adv. Mater.* 20 (2008) 4509–4512.
- [7] V. Leon, R. Parret, R. Almairac, L. Alvarez, M.-R. Babaa, B.P. Doyle, et al., Spectroscopic study of double-walled carbon nanotube functionalization for preparation of carbon/epoxy composites, *Carbon* 50 (2012) 4987–4994.
- [8] I.Y. Jang, H. Muramatsu, K.C. Park, Y.J. Kim, M. Endo, Capacitance response of double-walled carbon nanotubes depending on surface modification, *Electrochem. Commun.* 11 (2009) 719–723.
- [9] M. Pumera, Electrochemical properties of double wall carbon nanotube electrodes, *Nanoscale Res. Lett.* 2 (2007) 87–93.
- [10] Ü. Anik, S. Çevik, Double-walled carbon nanotube based carbon paste electrode as xanthine biosensor, *Microchim. Acta* 166 (2009) 209–213.
- [11] F. Rumiche, H.H. Wang, J.E. Indacochea, Development of a fast-response/high-sensitivity double wall carbon nanotube nanostructured hydrogen sensor, *Sensor. Actuator. B* 163 (2012) 97–106.
- [12] Y.S. Al-Hamdani, D. Alfe, A. Michaelides, How strongly do hydrogen and water molecules stick to carbon nanomaterials? *J. Chem. Phys.* 146 (2017), 094701.
- [13] R.A. Bell, M.C. Payne, A.A. Mostofi, Does water dope carbon nanotubes? *J. Chem. Phys.* 141 (2014) 164703.
- [14] A. Lekawa-Raus, L. Kurzepa, G. Kpizowski, S.C. Hopkins, M. Wozniak, D. Lukawski, et al., Influence of atmospheric water vapour on electrical performance of carbon nanotube fibres, *Carbon* 87 (2015) 18–28.
- [15] P.C.P. Watts, N. Mureau, Z. Tang, Y. Miyajima, J.D. Carey, S.R.P. Silva, The importance of oxygen-containing defects on carbon nanotubes for the detection of polar and non-polar vapours through hydrogen bond formation, *Nanotechnology* 18 (2007) 1751701.
- [16] A. Zahab, L. Spina, P. Poncharal, C. Marlière, Water-vapor effect on the electrical conductivity of a single-walled carbon nanotube mat, *Phys. Rev. B* 62 (2000) 10000–10003.
- [17] D. Tang, L. Ci, W. Zhou, S. Xie, Effect of H₂O adsorption on the electrical transport properties of double-walled carbon nanotubes, *Carbon* 44 (2006) 2155–2159.
- [18] E. Contés-de Jesús, J. Li, C.R. Cabrera, Latest advances in modified/function-alized carbon nanotube-based gas sensors, in: S. Suzuki (Ed.), *Synthesis and Applications of Carbon Nanotubes and Their Composites*, IntachOpen, 2013, pp. 337–366.
- [19] S. Arunachalam, A.A. Gupta, R. Izquierdo, F. Nabki, Suspended carbon nanotubes for humidity sensing, *Sensors* 18 (2018) 1655.
- [20] C.L. Cao, C.G. Hu, L. Fang, S.X. Wang, Y.S. Tian, C.Y. Pan, Humidity sensor based on multi-walled carbon nanotube thin films, *J. Nanomater.* (2011) 707303.
- [21] M.D. Ellison, A.P. Good, C.S. Kinnaman, N.E. Padgett, Interaction of water with single-walled carbon nanotubes: reaction and adsorption, *J. Phys. Chem. B* 109 (2005) 10640–10646.
- [22] I.V. Anoshkin, A.G. Nasibulin, P.R. Mudimela, M. He, V. Ermolov, E.I. Kauppinen, Single-walled carbon nanotube networks for ethanol vapor sensing applications, *Nano Research* 6 (2013) 77–86.
- [23] Yu.V. Fedoseeva, L.G. Bulusheva, A.V. Okotrub, D.V. Vylikh, A. Fonseca, A comparative study of argon ion irradiated pristine and fluorinated single-wall carbon nanotubes, *J. Chem. Phys.* 111 (2010) 224706.
- [24] D. Erbahar, S. Berber, Chlorination of carbon nanotubes, *Phys. Rev. B* 85 (2012), 085426.
- [25] A. Desforges, A.V. Bridi, J. Kadok, E. Flahaut, F. Le Normand, J. Gleize, et al., Dramatic enhancement of double-walled carbon nanotube quality through a one-pot tunable purification method, *Carbon* 110 (2016) 292–303.
- [26] J. Barkauskas, I. Stankeviciene, A. Selskis, A novel purification method of carbon nanotubes by high-temperature treatment with tetrachloromethane, *Separ. Purif. Technol.* 71 (2010) 331336.
- [27] V.K. Abdelkader, S. Scelfo, C. García-Gallarrín, M.L. Godino-Salido, M. Domingo-García, F.J. López-Garzón, M. Pérez-Mendoza, Carbon tetrachloride cold plasma for extensive chlorination of carbon nanotubes, *J. Phys. Chem. C* 117 (2013) 16677–16685.
- [28] L. Oliveira, F. Lu, L. Andrews, G.A. Takacs, M. Mehan, T. Debies, UV photo-chlorination and bromination of single-walled carbon nanotubes, *J. Mater. Res.* 29 (2014) 239–246.
- [29] U. Dettlaff-Weglikowska, V. Skákalová, R. Graupner, S.H. Jhang, B.H. Kim, H.J. Lee, et al., Effect of SOCl₂ treatment on electrical and mechanical properties of single-walled carbon nanotube networks, *J. Am. Chem. Soc.* 127 (2005) 5125–5131.
- [30] R. Kaur, A.K. Paul, A. Deep, Conjugation of chlorinated carbon nanotubes with quantum dots for electronic applications, *Matter Letters* 117 (2014) 165–167.
- [31] E. Flahaut, R. Basca, A. Peigney, C. Laurent, Gram-scale CCVD synthesis of double-walled carbon nanotubes, *Chem. Commun.* (2003) 1442–1443.
- [32] E.V. Lobiak, L.G. Bulusheva, E.O. Fedorovskaya, Y.V. Shubin, P.E. Plyusnin, P. Lonchambon, et al., One-step chemical vapor deposition synthesis and supercapacitor performance of nitrogen-doped porous carbon-carbon nanotube hybrids, *Beilstein J. Nanotechnol.* 8 (2017) 2669–2679.
- [33] S. Osswald, E. Flahaut, H. Ye, Y. Gogotsi, Elimination of D-band in Raman spectra of double-wall carbon nanotubes by oxidation, *Chem. Phys. Lett.* 402 (2005) 422–427.
- [34] T. Bortolamiol, P. Lukanov, A.-M. Galibert, B. Soula, P. Lonchambon, L. Datas, E. Flahaut, Double-walled carbon nanotubes: quantitative purification assessment, balance between purification and degradation and solution filling as an evidence of opening, *Carbon* 78 (2014) 79–90.
- [35] N.F. Yudanov, A.V. Okotrub, L.G. Bulusheva, I.P. Asanov, Y.V. Shubin, L.I. Yudanov, et al., Layered compounds based on perforated graphene, *J. Struct. Chem.* 52 (2011) 903–909.
- [36] S.G. Stolyarova, E.S. Kobeleva, I.P. Asanov, A.V. Okotrub, L.G. Bulusheva, Effect of the graphite oxide composition on the structure of products obtained by sulfuric acid treatment at elevated temperatures, *J. Struct. Chem.* 58 (2017) 1180–1186.
- [37] L.G. Bulusheva, V.E. Arkhipov, E.O. Fedorovskaya, S. Zhang, A.G. Kurennya, M.A. Kanygin, et al., Fabrication of free-standing aligned multiwalled carbon nanotube array for Li-ion batteries, *J. Pow. Sour.* 311 (2016) 42–48.
- [38] M.V. Katkov, V.I. Sysoev, A.V. Gusev, I.P. Asanov, L.G. Bulusheva, A.V. Okotrub, A backside fluorine-functionalized graphene layer for ammonia detection, *Phys. Chem. Chem. Phys.* 17 (2015) 444–450.
- [39] J.P. Perdew, K. Burke, M. Ernzerhof, Generalized gradient approximation made simple, *Phys. Rev. Lett.* 77 (1996) 3865.
- [40] V. Zolyomi, J. Koltai, Á. Ruzsnyák, J. Kürti, Á. Gali, F. Simon, et al., Intershell interaction in double walled carbon nanotubes: charge transfer and orbital mixing, *Phys. Rev. B* 77 (2008) 245403.
- [41] D. Resenthal, M. Ruta, R. Schlogl, L. Kiwi-Minsker, Combined XPS and TPD study of oxygen-functionalized carbon nanofibers grown on sintered metal fibers, *Carbon* 48 (2010) 1835–1843.
- [42] H. Estrade-Szwarckopf, XPS photoemission in carbonaceous materials: a “defect” peak beside the graphitic asymmetric peak, *Carbon* 42 (2004) 1713–1721.
- [43] E.O. Fedorovskaya, L.G. Bulusheva, A.G. Kurennya, I.P. Asanov, A.V. Okotrub, Effect of oxidative treatment on the electrochemical properties of aligned multi-walled carbon nanotubes, *Russ. J. Electrochem.* 52 (2016) 441–448.
- [44] M. Zaka, Y. Ito, H. Wang, W. Yan, A. Robertson, Y.A. Wu, et al., Electron paramagnetic resonance investigation of purified catalyst-free single-walled carbon nanotubes, *ACS Nano* 4 (2010) 7708–7716.
- [45] J.-W. Jang, K.W. Lee, C.E. Lee, B. Kim, C.J. Lee, Differences in the catalyst removal from single- and double-walled carbon nanotubes, *Curr. Appl. Phys.* 13 (2013) 1069–1074.
- [46] Y.-Z. Tan, B. Yang, K. Parvez, A. Narita, S. Osella, D. Beljonne, et al., Atomically precise edge chlorination of nanographenes and its application in graphene nanoribbons, *Nat. Commun.* 4 (2013) 2646.
- [47] V.A. Tur, A.V. Okotrub, Yu.V. Shubin, B.V. Senkovskiy, L.G. Bulusheva, Chlorination of perforated graphite via interaction with thionylchloride, *Phys. Status Solidi B* 251 (2014) 2613–2619.
- [48] R. Tang, Y. Shi, Z. Hou, L. Wei, Carbon nanotube-based chemiresistive sensors, *Sensors* 17 (2017) 882.
- [49] P.E. Lyons, S. De, F. Blighe, V. Nicolosi, L.F.C. Pereira, M.S. Ferreira, J.N. Coleman, The relationship between network morphology and conductivity in nanotube films, *J. Appl. Phys.* 104 (2008), 044302.
- [50] A. Salehi-Khojin, F. Khalili-Araghi, M.A. Kuroda, K.Y. Lin, J.-P. Leburton, R.I. Masel, On the sensing mechanism in carbon nanotube chemiresistors, *ACS Nano* 5 (2011) 153–158.
- [51] K. Zhang, J. Zou, Q. Zhang, Roles of inter-SWCNT junctions in resistive humidity response, *Nanotechnology* 26 (2015) 455501.
- [52] D. Jung, M. Han, G.S. Lee, Humidity-sensing characteristics of multi-walled carbon nanotube sheet, *Mater. Lett.* 122 (2014) 281–284.
- [53] H. Bi, K. Yin, X. Xie, J. Ji, S. Wan, L. Sun, et al., Ultrahigh humidity sensitivity of graphene oxide, *Sci. Rep.* 3 (2013) 2714.
- [54] C. Cantalini, L. Valentini, I. Armentano, L. Lozzi, J.M. Kenny, S. Santucci, Sensitivity to NO₂ and cross-sensitivity analysis to NH₃, ethanol, and humidity of carbon nanotubes thin films prepared by PECVD, *Sensor. Actuator. B* 95 (2003) 195–202.
- [55] A. Desforges, G. Mercier, C. Hérold, J. Gleize, F. Le Normand, B. Vigolo, Improvement of carbon nanotube stability by high temperature oxygen/chlorine gas treatment, *Carbon* 76 (2014) 275–284.
- [56] O.K. Varghese, P.D. Kichambre, D. Gong, K.G. Ong, E.C. Dickey, C.A. Grimes, Gas sensing characteristics of multi-walled carbon nanotubes, *Sens. Actuators, B* 83 (2001) 32–41.
- [57] X. Huang, Y. Sun, L. Wang, F. Meng, J. Liu, Carboxylation multi-walled carbon nanotubes modified with LiClO₄ for water vapour detection, *Nanotechnology* 15 (2004) 1284–1288.
- [58] Y. Ling, G. Gu, R. Liu, X. Lu, V. Kayastha, C.S. Jones, et al., Investigation of the humidity-dependent conductance of single-walled carbon nanotube networks, *J. Appl. Phys.* 113 (2013), 024312.
- [59] J. Zhao, A. Buldum, J. Han, J.P. Lu, Gas molecule adsorption in carbon nanotubes and nanotube bundles, *Nanotechnology* 13 (2002) 195–200.
- [60] M. Abdali, S. Mirzakhaki, A band structure study on inter-wall conductance of double-walled carbon nanotubes, *Mater. Sci. Semicond. Process.* 17 (2014) 222–227.